spectrum have been made with the aid of normal-coordinate analysis.[26] Vibrational frequencies calculated at the Hartree-Fock level are known to be an average ~10% greater than the experimental frequencies for a wide range of molecules,[27] and therefore the frequencies calculated here are scaled by 0.9 for comparison with experiments. If one compares the set of scaled gas-phase frequencies with the solid-state experimental values, the agreement is significantly worse than one might have expected at that level of theory. However, vibrational frequencies calculated in a polar medium are in substantially better agreement. In particular, the deviations between theory and experiment for the ν_2, ν_5, and ν_{10} vibrational frequencies are reduced from 119, 188, and 159 cm^{-1}, respectively, to 16, 61, and 79 cm^{-1}.

Another interesting aspect related to the changes in vibrational frequencies is the assignment of vibrational modes. The assignments for the gas-phase and SCRF vibrational frequencies are the same except for the ν_4 and ν_5 absorption modes. These two bands are mixtures of N-S stretch and symmetric SO_3 deformation modes. In the gas phase, the ν_4 band is dominated by the N-S stretch, whereas in a polar medium it is predominantly an SO_3 deformation. The situation is exactly reversed for the ν_5 absorption peak. Therefore, the assignment of ν_5 (604 cm^{-1}) to the N-S stretch is consistent with the experimental assignment.[26] However, smaller value (ν_4 = 345 cm^{-1}) is predicted for N-S stretching frequency in the gas phase.

Figure 4 displays the calculated IR spectra of both the zwitterion (**1a**) and neutral form (**2a**) in the gas phase and polar medium. It is immediately apparent that the calculated IR intensities are substantially different. In general, most absorption peaks are more intense on going from vacuum to a polar medium, and the ratios of increase are about the same. Note that some decreases in intensity are observed. For instance, the intensity of the ν_4 absorption peak of the zwitterion is calculated to decrease significantly from 61 to 14 km mol^{-1}.

Conclusions

Several interesting points have been revealed by this study:

(1) In the gas phase, the zwitterionic form (staggered C_{3v}, **1a**) of sulfamic acid lies within 1 kcal mol^{-1} of the neutral acid form (gauche-HOSN C_1, **2a**). These two structures are separated by a barrier of 28.6 kcal mol^{-1}. Correction for electron correlation is essential in evaluating the relative stability of the zwitterion and neutral isomers.

(2) The binding energies of the zwitterion, relative to ammonia and sulfur trioxide, in the gas phase and in a polar medium are 19.1 and 32.6 kcal mol^{-1}, respectively. The N-S bond of the zwitterion exhibits characteristics of a shared interaction. Stronger covalent character is predicted for this N-S bond than the B-N bond of BH_3·NH_3.

(3) In agreement with experiment, the zwitterion is calculated to be the preferred structure in both nonpolar and polar condensed media. In a dielectric medium of ϵ = 40.0, the zwitterion is significantly more stable than the neutral form by 10.2 kcal mol^{-1}. On going from the gas phase to a polar medium, significant enhancement of the dipole moment (by 3 D) of the zwitterion is observed. Stronger covalent character is also predicted for the N-S bond.

(4) The discrepancy between the calculated and solid-state geometries of the zwitterion (**1a**), reported by Hickling and Woolley, has been resolved. It is the result of a genuine difference in structure between the gas phase and solid state. The N-S bond length is calculated to decrease by 0.10 Å from the gas phase to a dielectric medium of ϵ = 40.0, and the OSN angle is calculated to increase by 3°.

(5) The infrared spectra of both **1a** and **2a** are strongly influenced by the solvent reaction field. Large frequency shifts (up to 200 cm^{-1} and intensity changes are observed. The calculated frequencies are in better agreement with the solid-state experimental data when the reaction field is included.

(6) All the results, including the geometry changes, the changes in relative energies, and the changes in vibrational frequencies from gas phase to a polar medium, are in good accord with the experimental findings. This demonstrates that the reaction field model provides an adequate description of a compact dipolar molecule in any polarizable environment.

Acknowledgment. This research was supported by a grant from the National Institutes of Health and by Lorentzian, Inc. We thank Prof. P. v. R. Schleyer for a preprint of ref 20.

Registry No. NH_2SO_2OH, 5329-14-6.

(27) Pople, J. A.; Schlegel, H.; Krishnan, R.; DeFrees, D. J.; Binkley, J. S.; Frisch, J. A.; Whiteside, R. F.; Hout, R. F.; Hehre, W. J. *Int. J. Quantum Chem. Symp.* **1981**, *15*, 269.

Determination of Enantiomerization Barriers by Computer Simulation of Interconversion Profiles: Enantiomerization of Diaziridines during Chiral Inclusion Gas Chromatography

M. Jung and V. Schurig*

Contribution from the Institut für Organische Chemie der Universität, Auf der Morgenstelle 18, D-7400 Tübingen, Germany. *Received May 20, 1991*

Abstract: A new general computer program has been developed for the simulation of chromatograms featuring dynamic phenomena in chromatography. It has been applied to the determination of enantiomerization barriers by simulation of experimentally observed elution profiles of enantiomers interconverting during their separation on a chiral stationary phase in a chromatographic column. For two diaziridines interconversion profiles could be observed in inclusion gas chromatography using permethylated β-cyclodextrin dissolved in OV-1701 as stationary phase. The simulation obtained at different temperatures and pressures yielded $\Delta G^{\ddagger}_s$ in the stationary phase 1-4 kJ/mol lower than $\Delta G^{\ddagger}_m$ in the mobile phase. From the temperature dependence of $\Delta G^{\ddagger}_s$, the quantities $\Delta H^{\ddagger}_s$ and $\Delta S^{\ddagger}_s$ in the stationary phase have been determined. Furthermore, the concept of the retention increase R' (caused by the addition of the cyclodextrin to the achiral polysiloxane OV-1701) allowed a separation of the contributions of enantiomerization in the physically dissolved state on the one hand and in the complexed state of the enantiomers on the other hand to the overall enantiomerization barrier in the stationary phase, $\Delta G^{\ddagger}_s$.

In analogy to dynamic NMR spectroscopy,[1] dynamic chromatography has been introduced in recent years as a tool for the investigation of dynamic processes[2] and the determination of the corresponding rate constants[3-5] and has been applied to the in-

0002-7863/92/1514-529$03.00/0

vestigation of enantiomerization[6] phenomena.[7,8,10-14] If enantiomerization is at a suitable rate on the chromatographic time scale, the interconversion of configurationally labile enantiomers during chromatography yields plateaus between the peaks of the enantiomers separated on the chiral stationary phase.

Three models have been described as a theoretical basis for the simulation of dynamic chromatographic processes: (i) the discontinuous plate model,[2,15,16] (ii) the stochastic model, assuming a Gauss function for the elution at the end of the column,[17,18] and (iii) the continuous flow model.[2-5] There are several reports on the simulation of chromatograms, using the models i[8] in the GC mode and ii[12-14] or iii[3-5] in the HPLC mode. We have chosen our previous discontinuous theoretical plate model for the development of an improved, general computer program for the simulation of chromatograms because of its mathematical simplicity and the possibility of application to systems involving more complicated kinetics.[19] The program and the procedure described below may be employed for the determination of rate constants, energy barriers, and equilibrium constants of any reaction(s) occurring during chromatography, e.g., enantiomer or diastereomer interconversions or intermolecular chemical reactions.

The first example of an interconversion profile was obtained for 1-chloro-2,2-dimethylaziridine on a stationary phase containing a chiral metal complex (nickel(II) bis[3-(trifluoroacetyl)-(1*R*)-camphorate] in squalane) in complexation gas chromatography.[7,8] We now found that 1-isopropyl-3,3-dimethyldiaziridine (**1**) and 1,2,3,3-tetramethyldiaziridine (**2**) display characteristic interconversion profiles on permethylated β-cyclodextrin dissolved in the polysiloxane OV-1701 as a stationary phase in inclusion gas chromatography.[20]

Results

Discontinuous Plate Model. We have now developed an improved version of the model previously employed.[8] The chromatographic separation is described as a discontinuous process by assuming that all processes proceed repeatedly in separate

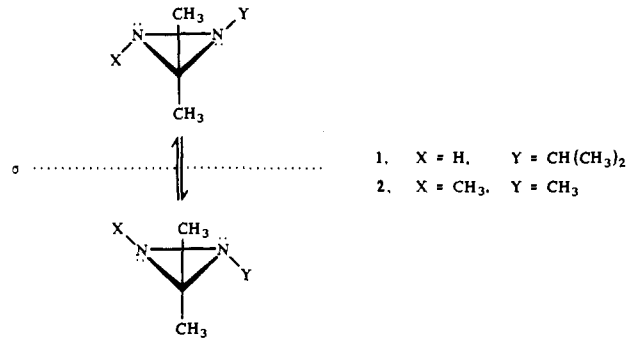

uniform sections of a multicompartmentalized column containing n theoretical plates considered as chemical reactors. Every section (theoretical plate) contains both a mobile and a stationary phase. The processes taking place in the chromatographic column are separated into three steps: (i) establishment of the distribution (partitioning) equilibrium of all species between mobile and stationary phase, (ii) reactions between the species during the time period Δt (here, reversible first-order interconversion of the enantiomers A and B in both phases with the respective rate constants), and (iii) transportation (shifting) of the mobile phase to the adjacent section of the column while the stationary phase is retained. The species are initially "injected" into the mobile phase of the first plate (initial amounts of substance in moles), and the content of the mobile phase of the last section is recorded in a digitalized form (eluted amount of substance per time in moles per minute) after every mobile phase shift. Significantly, peak broadening caused by the chromatographic process is an integral part of the plate model employed here. The number of species is no longer limited to two[8] in order to make the new computer program[19] applicable to multicomponent systems. Furthermore, the previous restriction that interconversions of the species are not taking place in the mobile phase[8] has been abandoned.

The distribution equilibria of the enantiomers A and B between the mobile and stationary phase in a theoretical plate are described by

$$a_m = \frac{1}{1 + k'_A}(a_m^\circ + a_s^\circ) \qquad b_m = \frac{1}{1 + k'_B}(b_m^\circ + b_s^\circ) \quad (1)$$

$$a_s = \frac{k'_A}{1 + k'_A}(a_m^\circ + a_s^\circ) \qquad b_s = \frac{k'_B}{1 + k'_B}(b_m^\circ + b_s^\circ) \quad (2)$$

where a_m, b_m, a_s, and b_s are the amounts of substance (not concentrations) of enantiomers A and B, respectively, in the mobile and stationary phase at equilibrium, a_m°, b_m°, a_s°, and b_s° are the molar amounts of substance before the equilibration, and k'_A and k'_B are the capacity factors of A and B (calculated from the retention time t_R and the dead time[21] t_M according to $k' = (t_R - t_M)/t_M$).

Enantiomerization. Contrary to dynamic NMR spectroscopy, an inherent prerequisite of the study of any interconversion equilibria by chromatography is the distribution of the solutes A and B between a mobile phase and a stationary phase capable of quantitatively resolving A and B (here, a chiral stationary phase capable of resolving the enantiomers). The reversible first-order enantiomerization of the enantiomers A and B occurs with different rate constants k^m and k^s in the mobile and stationary phase according the the following scheme:[8]

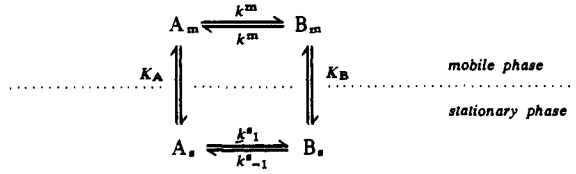

where K_A and K_B represent the ratio of concentration in the

(1) Jackman, L. M., Cotton, F. A., Eds. *Dynamic NMR Spectroscopy*; Academic Press: New York, 1975.
(2) Langer, S. H.; Yurchak, J. Y.; Patton, J. E. *Ind. Eng. Chem.* **1969**, *61*, 11-21.
(3) Melander, W.; Lin, H.-J.; Horvath, C. *J. Phys. Chem.* **1984**, *88*, 4527-4536.
(4) Jacobson, J.; Melander, W.; Vaisnys, G.; Horvath, C. *J. Phys. Chem.* **1984**, *88*, 4536-4542.
(5) Henderson, D. E.; Horvath, C. *J. Chromatogr.* **1986**, *368*, 203-213.
(6) As previously,[7,8] we define enantiomerization a *reversible* interconversion of the enantiomers, i.e., (+) ⇌ (-) (k), while racemization is often considered an *irreversible* transformation of one of the enantiomers into a racemic modification,[9a] i.e., (+) → (±) (k'), where $k' = 2k$,[9b] since the interconversion of one molecule reduces the enantiomer excess (ee) by two molecules.
(7) Schurig, V.; Bürkle, W. *J. Am. Chem. Soc.* **1982**, *104*, 7573-7580.
(8) Bürkle, W.; Karfunkel, H.; Schurig, V. *J. Chromatogr.* **1984**, *288*, 1-14.
(9) (a) Mislow, K. *Introduction to Stereochemistry*; W. A. Benjamin, Inc.: Reading, MA, 1965. (b) Eliel, E. L. *Stereochemistry of Carbon Compounds*; McGraw-Hill Book Co., Inc.: New York, 1962; p 33.
(10) Mannschreck, A.; Zinner, H.; Pustet, N. *Chimia* **1989**, *43*, 165-166.
(11) Mannschreck, A.; Kiessl, L. *Chromatographia* **1989**, *28*, 263-266.
(12) Stephan, B.; Zinner, H.; Kastner, F.; Mannschreck, A. *Chimia* **1990**, *44*, 336-338.
(13) Zinner, H. Doctoral Thesis, University of Regensburg, Germany, 1990, Chapter 8.
(14) Veciana, J.; Crespo, M. I. *Angew. Chem.* **1991**, *103*, 85-88; *Angew. Chem., Int. Ed. Engl.* **1991**, *30*, 74.
(15) Kallen, J.; Heilbronner, E. *Helv. Chim. Acta* **1960**, *43*, 489-500.
(16) Basset, D. W.; Habgood, H. W. *J. Phys. Chem.* **1960**, *64*, 769-773.
(17) Keller, H. A.; Giddings, J. C. *J. Chromatogr.* **1960**, *3*, 205-220.
(18) Kramer, R. *J. Chromatogr.* **1975**, *107*, 241-252.
(19) The program, written in FORTRAN 77, is available from us upon request and has been accepted by the Quantum Chemistry Program Exchange (QCPE). An application of a variation of the described program to a problem requiring a Runge-Kutta procedure for the kinetic calculations will be discussed in a forthcoming communication. A special procedure in the new program now allows some species to experience less theoretical plates than others (in this case, for some species the establishment of the distribution equilibrium is omitted in certain plates, and the resulting loss in retention is compensated by adding the amount of stationary phase of these plates to that of the previous plates).
(20) For a recent review, see: Schurig, V.; Nowotny, H.-P. *Angew. Chem.* **1990**, *102*, 969-986; *Angew. Chem., Int. Ed. Engl.* **1990**, *29*, 939.
(21) Gas chromatographic nomenclature according to ASTM; see: Ettre, L. S. *J. Chromatogr.* **1979**, *165*, 235-256.

stationary phase vs concentration in the mobile phase.

The residence time Δt in a theoretical plate between two mobile phase shifts is calculated from the dead time t_M and the number of plates n into which the column is divided according to

$$\Delta t = t_M/n \tag{3}$$

For enantiomers, the forward and backward rate constants k^m in the (achiral) mobile phase must be equal (i.e., the equilibrium constant is $K^m = 1$), whereas in the stationary phase the equilibrium constant $K^s = k^s_1/k^s_{-1}$ is determined by the two phase distribution coefficients K_A and K_B according to the principle of microscopic reversibility for $K^m = 1$[8]

$$K^s = k^s_1/k^s_{-1} = K_B/K_A = k'_B/k'_A \tag{4}$$

where k'_A and k'_B are the capacity factors of the enantiomers A and B, related with the phase distribution coefficients over the phase ratio β[21] according to $K = \beta k'$. This means that k^s_{-1} is already determined for given values of k^s_1, k'_A, and k'_B. An important consequence of eq 4 is that $k^s_1 \neq k^s_{-1}$ if enantiomer separation occurs ($K_A \neq K_B$); i.e., the forward and backward rate constants of enantiomerization become different in the presence of the chiral stationary phase. Note, however, that no enantiomer enrichment is involved in the overall process since the enantiomer interconverting at a lower rate has a longer residence time in the stationary phase. The reversible first-order kinetics is described by[8]

$$a_s = \frac{k^s_{-1}(a_s^\circ + b_s^\circ) - (k^s_{-1}b_s^\circ - k^s_1 a_s^\circ)e^{-(k^s_1+k^s_{-1})\Delta t}}{k^s_1 + k^s_{-1}} \tag{5}$$

(and analogously for b_s, a_m, and b_m, using the corresponding rate constants) where a_s and a_s° may be either the amounts of substance or concentrations of solute A in the mobile phase after and before the time interval Δt, etc.

The theoretical plate model[8] has been extended to the simulation of dynamic processes occurring in both the mobile and stationary phase. The rate constants of enantiomerization may be similar in both phases[13,14] or significantly different, as for 1-chloro-2,2-dimethylaziridine in complexation gas chromatography, where an activating effect of the metal complex renders enantiomerization in the stationary phase[8] 40 times faster than in the mobile phase.[22] The interconversion profile (plateau) is influenced by the rate constants of both phases according to the residence times of the enantiomers A and B in the two phases, which is quantitatively expressed by the capacity factors k', and the overall rate constants k_1 and k_{-1} can thus be defined:[14]

$$k_1 = \frac{1}{1 + k'_A}k^m + \frac{k'_A}{1 + k'_A}k^s_1$$
$$k_{-1} = \frac{1}{1 + k'_B}k^m + \frac{k'_B}{1 + k'_B}k^s_{-1} \tag{6}$$

The simulation procedure furnishes the overall rate constants k_1 and k_{-1}. If k^m and k^s_1 are not too different, k_1 and k_{-1} can be directly used for the simple and convenient estimation of enantiomerization barriers $\Delta G^\ddagger \approx \Delta G^\ddagger_m$.[14] If k^m is already known from independent measurements, or is negligible,[8] k^s_1 can be calculated according to eq 6.

Mannschreck et al.[23,24] determined the enantiomerization barriers ($\Delta G^\ddagger$) in solution for various diaziridines and oxaziridines by NMR and polarimetry (after preparative optical enrichment) in the same temperature range as that used here for the chromatographic simulations. Since they found only very little dependence on the choice of the solvent and the temperature, it seems reasonable to use these $\Delta G^\ddagger$ values for the estimation of approximate k_m values for the diaziridines **1** and **2** in the gas phase throughout the temperature range from 75 to 95 °C. For diaziridines, where two consecutive nitrogen inversions must occur during enantiomerization (the cis intermediate is not stable),[23,25] a statistical transmission coefficient $f = {}^1/_2$ has to be used[26] in the calculation of $\Delta G^\ddagger$ for a single nitrogen inversion from the rate constants of the overall process.[23,27] Therefore, this factor has been applied throughout.

The results of the simulation experiments are listed in Table II and shown in Figures 1 and 2. An excellent agreement of simulated and experimental chromatograms has been achieved. Figure 3 shows an enlarged peak profile with the separate elution

Table I. Experimental Retention Times t_M and t_R[a] and Retention Increases R'[b] for 1-Isopropyl-3,3-dimethyldiaziridine (**1**) and 1,2,3,3-Tetramethyldiaziridine (**2**) on 0.07 mol/kg Permethylated β-Cyclodextrin in OV-1701 as a Stationary Phase[c]

	temp (°C)					
	1					**2**
	75	80	85	90	95	80
retention times (min)[d]						
dead time t_M[e]	2.77	2.79	2.82	2.86	2.89	5.19
t_{R_A}	7.22	6.36	5.76	5.30	4.91	8.05
t_{R_B}	7.54	6.59	5.92	5.42	5.00	8.24
retention increases[f]						
R'_A	0.27	0.25	0.24	0.22	0.20	0.13
R'_B	0.35	0.32	0.30	0.27	0.25	0.19

[a] Used as a basis for the simulation shown in Figures 1 and 2; for data, see Table II. [b] Used for the determination of k^c; see Table III. [c] Inlet pressure 0.8 bar of H_2 for **1**, 0.5 bar for **2**. [d] ±0.02 min. [e] Methane. [f] ±2%, measured by using an achiral reference column, cf. Experimental Section. Due to a systematic error caused by interactions between the inert reference standard and the cyclodextrin, the true R' values may be ~0.1 higher.[29]

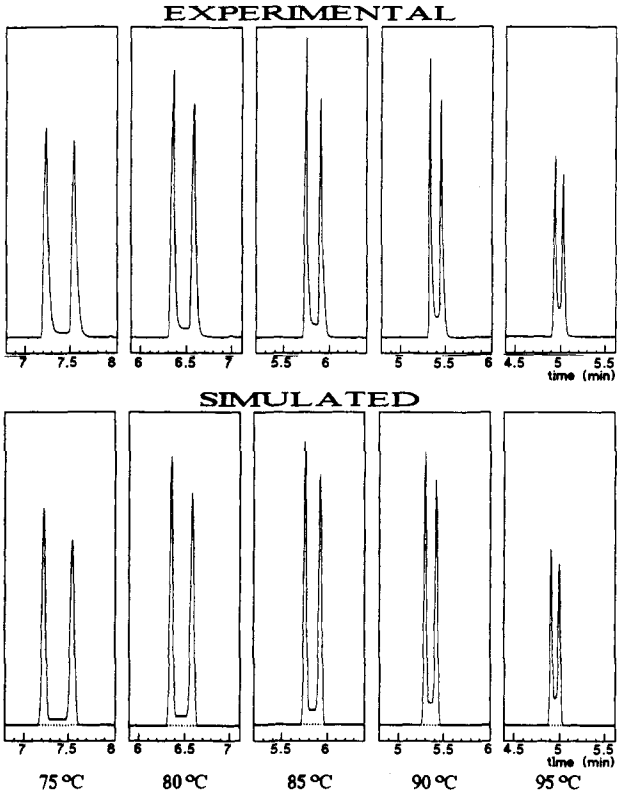

Figure 1. Experimental and simulated gas chromatograms of 1-isopropyl-3,3-dimethyldiaziridine (**1**) on 0.07 mol/kg permethylated β-cyclodextrin in OV-1701 at different temperatures (inlet pressure 0.8 bar of H_2). Plate number n used for the simulation: 85 000.

(22) Schurig, V.; Leyrer, U. *Tetrahedron: Asymmetry* **1990**, *1*, 865–868.
(23) Häkli, H.; Mintas, M.; Mannschreck, A. *Chem. Ber.* **1979**, *112*, 2028–2038.
(24) Mannschreck, A.; Seitz, W. *IUPAC, XXIIIrd International Congress of Pure and Applied Chemistry*; Butterworths: London, 1971; Vol. 2, p 309.
(25) Haselbach, E.; Mannschreck, A.; Seitz, W. *Helv. Chim. Acta* **1973**, *56*, 1614–1620.
(26) This is due to the fact that only half of the intermediate is transformed to the product while the other half reacts back to the starting material.
(27) Anderson, J. E.; Lehn, J. M. *J. Am. Chem. Soc.* **1967**, *89*, 81–87.

Table II. Rate Constants of Enantiomerization[a] k (min^{-1}) and the Corresponding Enantiomerization Barriers[b] $\Delta G^{\ddagger}$ (kJ/mol) for 1-Isopropyl-3,3-dimethyldiaziridine (**1**) and 1,2,3,3-Tetramethyldiaziridine (**2**) on 0.07 mol/kg Permethylated β-Cyclodextrin in OV-1701 as Stationary Phase[c]

	temp (°C)					
	1					**2**
	75	80	85	90	95	80
overall[d]						
k_1	0.0128	0.0164	0.021	0.032	0.051	0.0022
k_{-1}	0.0125	0.0158	0.021	0.031	0.050	0.0022
$\Delta G^{\ddagger}$ (±0.5)	108.2	109.1	109.9	110.2	110.4	115.0
mobile phase[e]						
k^m	0.0048	0.0084	0.0145	0.025	0.041	0.0011
$\Delta G^{\ddagger}_m$ (±0.7)	111.0	111.0	111.0	111.0	111.0	117.0
stationary phase[f]						
k^s_1	0.018	0.023	0.028	0.041	0.065	0.0042
k^s_{-1}	0.017	0.021	0.026	0.039	0.063	0.0040
$\Delta G^{\ddagger}_s$ (±1.0)	107.3	108.2	109.1	109.5	109.6	113.1

[a] For two consecutive nitrogen inversions, converting the *trans*-diaziridine into the enantiomeric *trans*-diaziridine via a cis intermediate (see text). [b] For a single nitrogen inversion, converting the *trans*-diaziridine into a cis intermediate (see text); calculated from the corresponding rate constants as described in the Experimental Section. [c] Inlet pressure 0.8 bar of H_2. [d] Obtained by simulation (see Figures 1 and 2) and comparison to the experimental elution profiles. [e] Approximate data according to the literature [23,24] (see text). [f] Obtained from the overall data and those for the mobile phase according to eq 6.

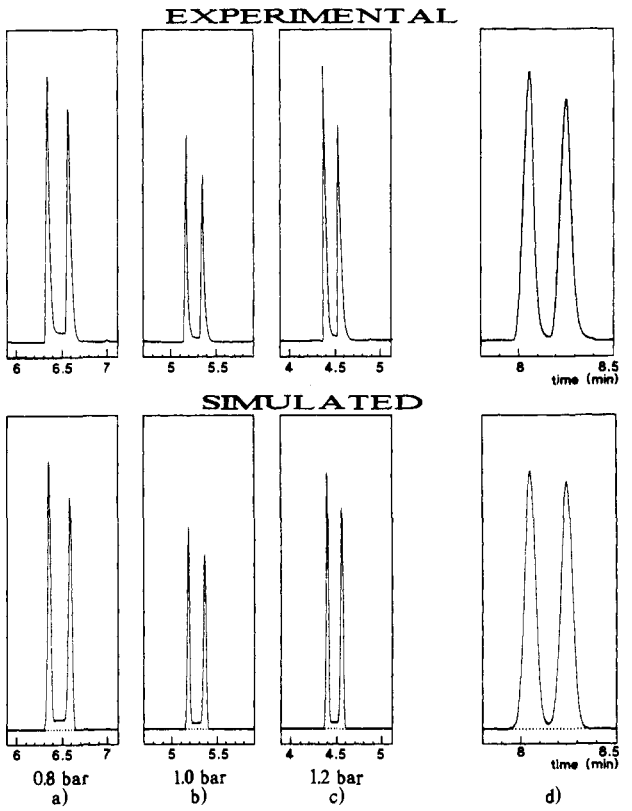

Figure 2. Experimental and simulated gas chromatograms of 1-isopropyl-3,3-dimethyldiaziridine (**1**) and 1,2,3,3-tetramethyldiaziridine (**2**) on 0.07 mol/kg permethylated β-cyclodextrin in OV-1701 at 80 °C: (a–c) **1** at different inlet pressures; (d) **2** at 0.5 bar of H_2 (showing a low but definite formation of a plateau). Plate number n used for the simulation: (a) 85 000, (b) 99 000, (c) 77 000, (d) 33 000.

curves of the enantiomers A and B.

Pressure Dependence. While the rate constants of the first-order enantiomerization do not depend on the flow rate in the column, i.e., the inlet pressure, the interconversion profiles do, which is due to the variation of the time spent in the column. Therefore, interconversion profiles simulated at different inlet pressures should yield the same rate constants. This has indeed been found: the good agreement of experimental and simulated chromatograms for different inlet pressures (see Figure 2, simulations based on the same rate constants throughout) supports our approach.

Temperature Dependence. Approximate values of $\Delta H^{\ddagger}_s$ and $\Delta S^{\ddagger}_s$ have been obtained from an Eyring plot ($\Delta G^{\ddagger}_s/T$ vs $1/T$,

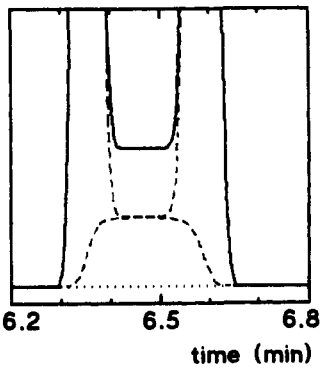

Figure 3. Enlargement of a simulated chromatogram of **1** at 80 °C (0.8 bar) (from Figure 1), showing the separate elution curves for the enantiomers.

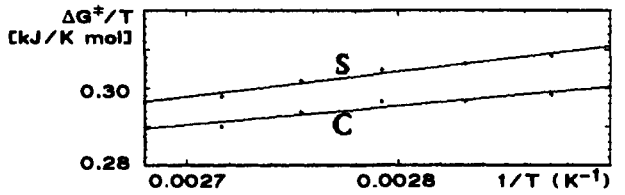

Figure 4. Eyring plots for **1** in the stationary phase (S) (i.e., $\Delta G^{\ddagger}_s/T$ vs $1/T$) and for **1** in the complexed state (C) within the stationary phase (i.e., $\Delta G^{\ddagger}_c/T$ vs $1/T$); data from Tables II and III; linear regression yields the $\Delta H^{\ddagger}_s$, $\Delta S^{\ddagger}_s$, $\Delta H^{\ddagger}_c$, and $\Delta S^{\ddagger}_c$ values given in the text.

Table III. Rate Constants of Enantiomerization[a] (min^{-1}) and the Corresponding Enantiomerization Barriers[b] $\Delta G^{\ddagger}$ (kJ/mol) for 1-Isopropyl-3,3-dimethyldiaziridine (**1**) and 1,2,3,3-Tetramethyldiaziridine (**2**) While Complexed (cf. Text) by Permethylated β-Cyclodextrin[c]

	temp (°C)					
	1					**2**
	75	80	85	90	95	80
k^c_1	0.065	0.080	0.084	0.12	0.19	0.029
k^c_{-1}	0.050	0.062	0.065	0.09	0.15	0.019
$\Delta G^{\ddagger}_c$ (±2.5)	104	105	106	107	107	108

[a] For two consecutive nitrogen inversions, converting the *trans*-diaziridine into the enantiomeric *trans*-diaziridine via a cis intermediate (see text). [b] For a single nitrogen inversion, converting the *trans*-diaziridine into a cis intermediate (see text); calculated from the corresponding rate constants as described in the Experimental Section. [c] 0.07 mol/kg solution in OV-1701 used as stationary phase; inlet pressure 0.8 bar of H_2. The data were obtained from those in Table II using the retention increases R' in Table I according to eq 7.

see Figure 4). These values are, however, inherently much less accurate than the $\Delta G^{\ddagger}_s$ values. For diaziridine **1** in the stationary phase, the temperature dependence of $\Delta G^{\ddagger}_s$ yields $\Delta H^{\ddagger}_s = 65 \pm 7$ kJ/mol and $\Delta S^{\ddagger}_s = -0.12 \pm 0.03$ kJ/(K·mol).

The Concept of the Retention Increase R'. If a chiral additive, e.g., a cyclodextrin, which is dissolved in an achiral solvent, e.g., a polysiloxane, is used as a stationary phase, the enantiomer will spend part of its time physically dissolved and part of its time complexed by the cyclodextrin. Thus, a more detailed reaction scheme can be formulated which distinguishes two dynamic phenomena within the stationary phase, i.e., enantiomerization in the dissolved (k^d) vs complexed state (k^c):

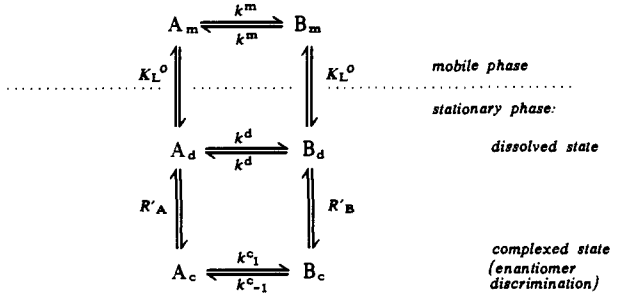

The retention increase R', i.e., $R' = (k'/k'_{achiral}) - 1$, is experimentally easily accessible (obtained by relating the retention parameters with those observed on an achiral reference column containing only the solvent devoid of the additive) and is a measure for the interaction between the enantiomer and the additive (in this case, the cyclodextrin (CD)), as expressed by the formation constant $K_{CD\cdot A}$ (given in terms of molality).[28,29] The retention increase R'_A of enantiomer A is defined as $R'_A = K_{CD\cdot A} m_{CD}$ (where m_{CD} is the molality of the cyclodextrin in the stationary phase) and thus represents the fraction of the complexed vs dissolved (uncomplexed) enantiomer A in the stationary phase,[28,29] i.e., $1/(R'_A + 1)$ and $R'_A/(R'_A + 1)$ are the fractions of residence time of A in the complexed and dissolved state within the stationary phase. Thus, an equation analogous to eq 6 can be written for enantiomers A and B in the stationary phase:

$$k^s_1 = \frac{1}{1 + R'_A} k^d + \frac{R'_A}{1 + R'_A} k^c_1$$
$$k^s_{-1} = \frac{1}{1 + R'_B} k^d + \frac{R'_B}{1 + R'_B} k^c_{-1} \qquad (7)$$

If we assume that, due to the little solvent dependence mentioned above, the rate constant of enantiomerization for the physically dissolved state in the stationary phase k^d is approximately equal to that in the mobile phase, k^m, eq 7 allows an estimation of the enantiomerization barrier in the complexed state, $\Delta G^{\ddagger}_c$, and an activating effect of the cyclodextrin can thus be evaluated (see Table III). Approximate values of $\Delta H^{\ddagger}_c$ and $\Delta S^{\ddagger}_c$ have been obtained from an Eyring plot ($\Delta G^{\ddagger}_c/T$ vs $1/T$, see Figure 4). The resulting (very rough) values for **1** are $\Delta H^{\ddagger}_c = 50 \pm 18$ kJ/mol and $\Delta S^{\ddagger}_c = -0.16 \pm 0.05$ kJ/(K·mol) in the complexed state (inclusion).

Discussion

Activating Effect of the Cyclodextrin. Using the rate constants of enantiomerization determined by Mannschreck et al.[23,24] for the estimations of k^m values for **1** and **2** in the mobile phase, the data listed in Table II clearly show that the rate constants in the stationary phase k^s are higher, but are still within the same order of magnitude as the rate constants in the mobile phase k^m. The k^c values for the complexed state, which are independent from the cyclodextrin molality in the stationary phase and thus of more general interest, although less accurate, are even higher (about 4–20 times as high as the corresponding rate constants in the gas phase). Obviously, cyclodextrins exert a significant activating effect on the rate of enantiomerization, although smaller than that reported for 1-chloro-2,2-dimethylaziridine in complexation gas chromatography[8,22] (activating effect by the metal in the stationary phase). However, since the retention increase R' is rather low for cyclodextrin stationary phases,[29] compared with those observed in complexation GC (i.e., the enantiomers spend much of their time in the stationary phase being physically dissolved in the polysiloxane and not complexed by the cyclodextrin), the influence of the activating effect of the cyclodextrin on the observed rate constants k_1 and k_{-1} is relatively small. Thus, the overall rate constants k_1 and k_{-1} are found to be only about 1.2–3 times as large as the corresponding k^m values and the enantiomerization barriers $\Delta G^{\ddagger}$ are lower only by 1–3 kJ/mol. Hence, the described method, employing gas chromatography of interconverting enantiomers on cyclodextrin stationary phases, provides an easy way of determining approximate enantiomerization barriers $\Delta G^{\ddagger}$ also for compounds of which the rate constants k^m in the mobile phase are not known. This reasoning is in agreement with results found in HPLC using (+)-poly(triphenylmethyl methacrylate)[14] and triacetylcellulose[12,13] as stationary phases.

Precision. According to the Eyring equation, $\Delta G^{\ddagger}$ values are significantly more precise than the corresponding rate constants; e.g., a rate constant of 0.05 $min^{-1} \pm 10\%$ would only produce an error of 0.4 kJ/mol in the corresponding $\Delta G^{\ddagger}$. The overall rate constants k_1 and k_{-1} and the corresponding overall $\Delta G^{\ddagger}$ can be determined quite precisely, but as described above, only overall values are obtained which depend on the individual values for the mobile (k^m) and the stationary phase (k^s). The determination of k^s_1 and k^s_{-1} according to eq 6 is subject to possible errors in k^m, obtained by independent measurements.

The rate constants for the complexed state k^c_1 and k^c_{-1} only represent semiquantitative figures since the reaction scheme on which eq 7 is based might still be a somewhat simplified model and since an error of the retention increase R'[29] used in eq 7 is introduced.

Conclusion

Computer simulation of experimental interconversion profiles (dynamic chromatography) is a simple and straightforward method for the determination of enantiomerization barriers. As demonstrated for the diaziridines **1** and **2**, deviations of the overall barriers (obtained by the simulation method) from barriers obtained by other methods are small if permethylated cyclodextrin is employed as chiral additive to the stationary phases. The method advanced here is particularly suitable for the determination of enantiomerization barriers in the range of ~70–130 kJ/mol where dynamic NMR techniques cannot be applied. Only trace amounts of the racemic sample are required (no need for tedious enantiomer enrichment). The method can also be applied to related dynamic phenomena such as epimerization, diastereomerization, or intermolecular chemical reactions.

Experimental Section

1-Isopropyl-3,3-dimethyldiaziridine (1) and 1,2,3,3-tetramethyldiaziridine (2) were obtained from Prof. Dr. A. Mannschreck, Regensburg, Germany.[23,25,30]

Gas Chromatography. A commercial fused silica capillary column (50 m × 0.25 mm i.d.) coated with 0.25-μm OV-1701 containing 0.07 mol/kg permethylated β-cyclodextrin was used (Chrompack, Middelburg, The Netherlands).[20] Hydrogen was used as a carrier gas. The measurements were performed on a Carlo-Erba MEGA gas chromatograph equipped with a flame-ionization detector and a Shimadzu C-R 3A integrator.

Computer Simulation. The calculations were performed on a CONVEX C 220.[19] The following data taken from the experimental chromatograms were used as a basis for the simulation: the dead time t_M, the retention times t_{R_A} and t_{R_B}, and the theoretical plate numbers n_A and n_B, the latter being practically equal. The initial amounts of the enantiomers A and B were equal (racemate). Given the rate constants k^m in the mobile phase, the simulation experiment was performed for different values of the rate constant k^s_1 in the stationary phase (k^s_{-1} being calcu-

(28) Schurig, V.; Chang, R. C.; Zlatkis, A.; Feibush, B. *J. Chromatogr.* **1974**, *99*, 147–171.

(29) Jung, M.; Schmalzing, D.; Schurig, V. *J. Chromatogr.* **1991**, *552*, 43–57.

(30) Mannschreck, A.; Radeglia, R.; Gruendemann, E.; Ohme, R. *Chem. Ber.* **1967**, *100*, 1778–1785.

lated from k^s_1 according to eq 4) in order to find the best agreement of simulated and experimental curves. Another possible procedure, yielding the same results, is to perform the simulation experiments for different values of k_1, to calculate k_{-1} from k_1 in agreement with eqs 4 and 6, i.e.

$$k_{-1} = k_1(k'_A + 1)/(k'_B + 1) = k_1 t_{R_A}/t_{R_B} \quad \text{(i)}$$

initially assuming the same rate constants in both phases, i.e., $k^m = {}^1/_2(k^s_1 + k^s_{-1}) = {}^1/_2(k_1 + k_{-1})$, in order to obtain k_1 and k_{-1}, and then to evaluate according to eq 6. $\Delta G^\ddagger$ was calculated from the corresponding rate constant k (mean of forward and backward reaction) according to the Eyring equation

$$k = f\frac{k_B T}{h} e^{-\Delta G^\ddagger/RT} \quad \text{(ii)}$$

where the transmission coefficient is $f = 0.5$ for two consecutive inversions[23,26] (cf. remarks in the text). An estimated error is given for the $\Delta G^\ddagger$ values.

Determination of Retention Increases R'. The retention increases R' were determined by using an achiral OV-1701 reference column, using *n*-octane as a reference standard, as previously described in detail.[7,28,29]

Acknowledgment. This work was supported by the Deutsche Forschungsgemeinschaft and Fonds der Chemischen Industrie. We thank Prof. Dr. A. Mannschreck, Regensburg, Germany, for supplying the diaziridines **1** and **2** and for valuable advice and discussions.

Registry No. 1, 137675-05-9; **2**, 137675-06-0.

Metallaoxetanes as Possible Intermediates in Metal-Promoted Deoxygenation of Epoxides and Epoxidation of Olefins

Jan-E. Bäckvall,*[1a] Fredrik Bökman,[1a] and Margareta R. A. Blomberg*[1b]

Contribution from the Department of Organic Chemistry, University of Uppsala, Box 531, 751 21 Uppsala, Sweden, and Department of Theoretical Physics, University of Stockholm, 113 46 Stockholm, Sweden. *Received May 31, 1991*

Abstract: Calculations including electron correlation have been performed for the insertion of a number of first and second row transition metal atoms (Cr, Co, Fe, Ni, Cu, Mo, Ag) into the C–O bond of ethene oxide. It is found that for all these metals, except silver, a metallacycle is more stable than the [metal + epoxide]. The energy of [metal + epoxide] is also compared to [metal oxide + ethene] and it is found that only for copper and silver is [metal + epoxide] lower in energy than [metal oxide + ethene]. The difference between the metals in this respect is explained by the difference in binding energy of the diatomic metal oxides. Silver and copper have much weaker M=O bonds than the rest of the metals studied, and this favors an epoxidation reaction.

Metallaoxetanes have been postulated as intermediates in epoxidation reactions with oxotransition metal complexes[2-4] and in metal-promoted deoxygenation of epoxides[2,5] (eq 1). Furthermore, they are likely intermediates in metal-catalyzed insertion of CO_2 into epoxides[6-8] and in the conversion of ketones to alkenes by metal–carbenes.[9-11] Several metallaoxetane complexes have been characterized,[11-13] and recently a ferraoxetane was observed in the matrix reaction between atomic iron and ethene oxide in argon at 12.5–15 K.[13]

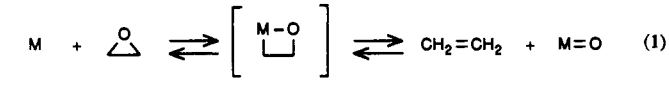

(1)

Table I. Calculated Energies in kcal/mol, Relative to the Ground State of the Metal Atom and Free Epoxide

metal atom	ground state	2-metalla-oxetane		open structure		metal oxide + ethene	
		state	ΔE	state	ΔE	state	ΔE
Cr	$^7S(d^5s)$	$^5A'$	−32			$^5\Pi$	−14
Fe	$^5D(d^6s^2)$	$^5A'$	−36	$^5A'$	+10	$^5\Sigma^+$	−16
		$^3A'$	−19				
Co	$^4F(d^7s^2)$	$^4A'$	−34	$^4A''$	+7	$^4\Delta$	−15
		$^2A''$	−30				
Ni	$^3D(d^9s)$	$^1A'$	−50	$^3A'$	−3	$^3\Sigma^-$	−18
Cu	$^2S(d^{10}s)$	$^2A'$	−17	$^2A'$	+3	$^2\Pi$	+13
Mo	$^7S(d^5s)$	$^5A'$	−35			$^5\Pi$	−26
Ag	$^2S(d^{10}s)$	$^2A'$	+12	$^2A'$	+17	$^2\Pi$	+35

In this paper we have performed quantum chemical calculations on 2-metallaoxetanes for a number of transition metals (Cr, Mo, Fe, Co, Ni, Cu, Ag) and compared the energy of the metallacycle with the energies of [metal + epoxide] and [metal oxide + ethene]. There are two important questions that we would like to address with these calculations: (i) is the metallaoxetane a likely intermediate in the transformations given in eq 1 and (ii) which is the preferred decomposition pathway for the metallacycle for a certain metal (epoxide or olefin).

The structure of the metallaoxetane used for the calculations is planar, and the geometrical parameters were optimized for the

(1) (a) University of Uppsala. (b) University of Stockholm.
(2) (a) Sharpless, K. B.; Teranishi, A. Y.; Bäckvall, J. E. *J. Am. Chem. Soc.* **1977**, *99*, 3120. (b) Rappé, A. K.; Goddard, III, W. A. *J. Am. Chem. Soc.* **1980**, *102*, 5114.
(3) (a) Jørgensen, K. A. *Chem. Rev.* **1989**, *89*, 431. (b) Jørgensen, K. A.; Schiøtt, B. *Chem. Rev.* **1990**, *90*, 1483.
(4) (a) Collman, J. P.; Kodadek, T.; Brauman, J. I. *J. Am. Chem. Soc.* **1986**, *108*, 2588. (b) Groves, J. T.; Watanabe, J. *J. Am. Chem. Soc.* **1986**, *108*, 507. (c) Groves, J. T.; Avaria-Neiser, G. E.; Fish, K. M.; Imachi, M.; Kuckowski, R. L. *J. Am. Chem. Soc.* **1986**, *108*, 3837.
(5) Sharpless, K. B.; Umbreit, M. A.; Nieh, M. T.; Flood, T. C. *J. Am. Chem. Soc.* **1972**, *94*, 6538.
(6) De Pasquale, R. J. *J. Chem. Soc., Chem. Commun.* **1973**, 157.
(7) Bäckvall, J. E.; Karlsson, O.; Ljunggren, S. O. *Tetrahedron Lett.* **1980**, *21*, 4985.
(8) Aye, K. T.; Gelmini, L.; Payne, N. C.; Vittal, J. J.; Puddephatt, R. J. *J. Am. Chem. Soc.* **1990**, *112*, 2464.
(9) Tebbe, F. N.; Parshall, G. W.; Reddy, G. S. *J. Am. Chem. Soc.* **1978**, *101*, 3611.
(10) (a) Pine, S. H.; Zahler, R.; Evans, D. A.; Grubbs, R. H. *J. Am. Chem. Soc.* **1980**, *102*, 3270. (b) Buchwald, S. L.; Grubbs, R. H. *J. Am. Chem. Soc.* **1983**, *105*, 5490.
(11) Bazan, G. C.; Schrock, R. R.; O'Regan, M. B. *Organometallics* **1991**, *10*, 1062.
(12) (a) Schlodder, J. A.; Ibers, J. A.; Lenarda, M.; Graziani, M. *J. Am. Chem. Soc.* **1974**, *96*, 6893. (b) Lenarda, M.; Pahor, N. B.; Calligaris, M.; Graziani, M.; Randaccio, L. *J. Chem. Soc., Dalton Trans.* **1978**, 279. (c) Lenarda, M.; Ros, R.; Traverso, O.; Pitts, W. D.; Baddley, W. H.; Graziani, M. *Inorg. Chem.* **1977**, *16*, 3178. (d) Ho, S. C.; Hentges, S.; Grubbs, R. H. *Organometallics* **1988**, *7*, 780.
(13) Kafafi, Z. H.; Hauge, R. H.; Billups, W. E.; Margrave, J. L. *J. Am. Chem. Soc.* **1987**, *109*, 4775.

0002-7863/92/1514-534$03.00/0